Multi-band/Multi-mode and Efficient Transmitter Based on a Doherty Power Amplifier

Paul Saad*, Luca Piazzon†, Paolo Colantonio†, Junghwan Moon‡, Franco Giannini†,
Kristoffer Andersson*, Bumman Kim‡, and Christian Fager*
*Department of Microtechnology and Nanoscience, Chalmers University of Technology,
Gothenburg, Sweden. Email: paul.saad@chalmers.se
†Department of Electronics Engineering, University of Roma Tor Vergata,
Roma, Italy. Email: luca.piazzon@uniroma2.it
‡Department of Electrical Engineering, Pohang University of Science and Technology,
Pohang, South Korea. Email: jhmoon@postech.ac.kr

***Abstract*—This paper presents the design of a high peak efficiency dual-band power amplifier (PA) and how it is adopted as basic cell to implement a high average efficiency Doherty PA (DPA), achieving a dual-band/multi-mode and efficient transmitter concurrently operating at 1.8 GHz and 2.4 GHz. From the dual-band PA, an average PAE of 25% has been experimentally obtained, when exited with concurrent 10MHz LTE and WiMAX signals. When using this PA as a basis for a dual band Doherty PA, the average PAE is improved (by 9 percentage units) to 34%. An adjacent channel leakage ratio (ACLR) lower than -46.5 dBc and -46.0 dBc has been fulfilled from PA and DPA, respectively, using a standard digital linearization technique.**

I. Introduction

'Multi-band', 'Multi-mode', and 'Efficient' are the most adopted adjectives to describe transmitters to be involved in the new communication systems [1]. 'Multi-band' transmitters allow operators to simultaneously support a combination of services at different frequency bands, while reducing cost, size, and number of devices. 'Multi-mode' transmitters allow operators to combine multiple access technologies such as 2G, 3G, and 4G onto a single platform. 'Efficient' transmitters allow operators to reduce energy cost, while increasing mobility as well as decreasing CO_2 emission [2]. A critical element in enabling the convergence of such capabilities in modern transmitters is the development of power amplifiers (PAs) that can be efficiently used across different frequency bands and for multi-standard applications.

Multi-band PAs were introduced in the 80s [3]. Efforts to obtain highly efficient multi-band PAs are gradually increased leading to the development of advanced solutions, mainly based on the harmonic manipulation concept [4]–[6]. However, the proposed techniques are not sufficient to fulfill multi-mode capability, maintaining satisfactory levels of efficiency. Such PAs, in fact, are not able to efficiently amplify signals presenting high peak to average ratio (PAR), as the ones commonly adopted in 3G and 4G systems.

An efficient amplification of signals presenting high PAR has been largely demonstrated adopting new PA architectures. Among them, the Doherty Power Amplifier (DPA) seems to be the most promising approach. The basic topology of the DPA [7] presents an intrinsic single-band behavior. Consequently, the implementation of multi-band DPAs became the new challenge for researchers in the last few years [8]–[11]. In fact, it is regarded as a realistic solution for the implementation of multi-band/multi-mode and efficient transmitters.

In this paper, the development of a highly efficient dual-band/multi-mode transmitter based on the DPA architecture is presented. The dual-band capability is achieved by designing a concurrent 1.8-2.4 GHz PA, whose efficiency is maximized by adopting the harmonic tuning approach described in Section II. Then, two of the dual-band PAs are properly combined to form a dual-band DPA as reported in Section III. The experimental results, reported in Section IV, based on both continuous wave and modulated signals, demonstrate the validity of the approach, highlighting both the improvements and the drawbacks when the DPA architecture is adopted.

II. Dual-Band PA Design

A 3.6mm bare-die GaN-HEMT from Cree (CGH60015DE) has been used for the design of the dual-band PA. Such a device presents a breakdown voltage of 100 V, a pinch-off voltage of -3.2 V, and a saturation drain current of 2.3 A. For the design, the nonlinear model of the device has been supplied by the manufacturer.

Multi-harmonic (up to the third) load-pull/source-pull simulations have been performed for each of the operating frequencies, 1.8 GHz and 2.4 GHz. Input and output loads to maximize the efficiency level have been, thus, inferred. Moreover, the effect of the harmonics on the efficiency performance has been studied as well. The results show that the effect on the performance from the second and third harmonics at the input and from the third harmonic at the output is minor [6]. Consequently, such harmonics have been neglected in the design of the respective networks, in order to reduce their complexity.

The output matching network has been designed in three steps. Firstly, the 2nd harmonics loading conditions have been achieved by using the approach proposed in [4]. Thus, obtaining the network framed within the box 'A' in Fig. 1, where the first ladder cell controls the 2nd harmonic of 2.4 GHz, while the second ladder cell controls the 2nd harmonic of

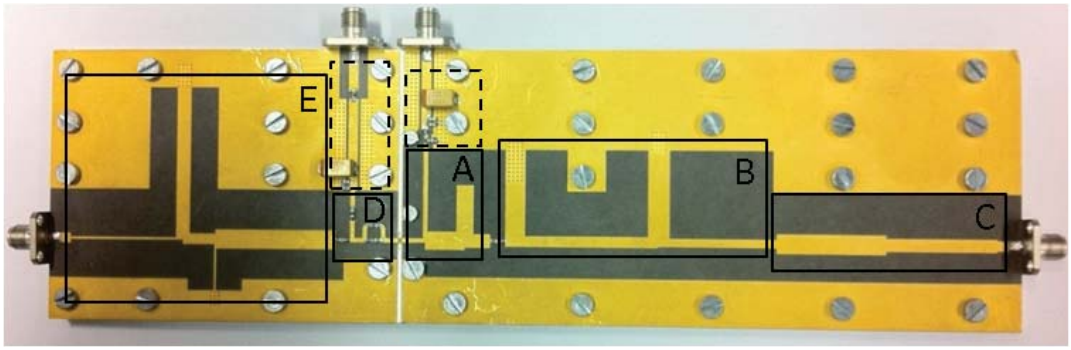

Fig. 1. Photos of the realized dual-band PA. Box 'A' is the network for the 2nd harmonics control. Box 'B' is the network for the synthesis of the reactive part of the loads at fundamentals. Box 'C' is the network for the transformation from the 50 Ohm termination to the optimum output resistance at the fundamentals. Box 'D' is the stabilization network. Box 'E' is the input matching network. Dashed boxed are the DC filtering networks.

1.8 GHz. After this step, the reactive parts of the load at the fundamentals have been synthesized by using the network framed within the box 'B' in Fig. 1. Obviously, the effect of the previously designed network for the harmonics control has been accounted for. Finally, the transformation from the 50 Ohm termination to the optimum output resistance has been fulfilled by adopting the method introduced in [12], resulting in the network framed within the box 'C' in Fig. 1.

The input network is composed by two parts. The stabilization network (box 'D' in Fig. 1) and the input matching network (box 'E' in Fig. 1). The latter has been designed to provide a 50 Ohm matched condition simultaneously at the two fundamental frequencies, with the aim to maximize the gain of the PA.

To complete the design, a low-pass filter has been added to each DC access point for the device biasing, in order to avoid loading effect from the supplier at radio frequencies. These networks are framed within dashed boxes in Fig. 1.

III. Dual-Band DPA Implementation

To implement the dual-band DPA, two dual-band PAs have been properly combined, obtaining the module reported in Fig. 2. The two PAs are framed within the boxes 'A' and 'B', realizing the Main and Auxiliary amplifiers, respectively. From both PAs, the network for the output resistance transformation (box 'C' in Fig. 1) has been removed, since this kind of dual-band transformer prevents a correct load modulation [11]. The two PAs have been connected at their output by means of a dual-band $\lambda/4$ (box 'C' in Fig. 2). To design this element, the topology proposed in [13] has been adopted. Moreover, its equivalent characteristic impedance ($Z_0 = 26$ Ohm) has been theoretically inferred following [14]. From [14], the output resistance ($R_L = 13$ Ohm) has been derived as well. As performed for the dual-band PA, the transformation from the 50 Ohm standard termination to the desired R_L has been obtained by using the approach proposed in [12]. The resulting network is framed within the box 'D' in Fig. 2.

At the input, the two dual-band PAs have been connected with a wide-band branch-line coupler. This solution has been preferred to a dual-band splitter to reduce the sensitivity of the module to the variations of the input capacitance, C_{gs}, of the active devices. In fact, due to the Class C bias condition, the value of C_{gs} of the Auxiliary amplifier is not accurately predicted by the model, which is validated up to the pinch-off voltage biasing condition only. The wide-band branch-line coupler is framed within the box 'E' in Fig. 2. It has been designed starting from [15] and then optimized to obtain the desired uneven splitting factor.

IV. Experimental results

Continuous wave (CW) measurements have been performed on both realized modules. Fig. 3 reports the frequency behaviors of output power, gain, and PAE at about 2 dB of gain compression. As expected, the DPA has shown a lower gain at the operating bands, due to the uneven input splitter. Moreover, the output power of the DPA is higher than the one of the PA, due to the doubled active periphery. Finally, the PAE of both modules is higher than 55% at both operating bands. These results demonstrate the capability of both designed PA and DPA to be adopted as efficient multi-band transmitter in 2G systems, that are based on phase modulated signals.

Comparing more accurately the behaviors in Fig. 3, one can note that the PA reaches equal levels of output power and PAE at both operating bands, while the DPA presents a performance reduction at the higher band. In fact, in terms of losses, the input/output combining networks of the DPA greatly affects the higher frequency. Moreover, the DPA has shown a higher sensitivity to the realization variances, due to the greater complexity of the circuit, as demonstrated by the little frequency shift on the output power peak. Also this phenomenon greatly affects the higher frequency. However, the greater complexity of the DPA does not affect the bandwidth. Similar levels of 1 dB gain ripple bandwidths have been, in fact, registered at both bands for both modules. Consequently, it is possible to declare that the combining structures added in the DPA are less critical for the bandwidth respect to the input/output matching networks of the PA.

The performance of the designed modules have also been tested by using signals usually adopted in 3G and 4G systems. In particular, both PA and DPA have been characterized in

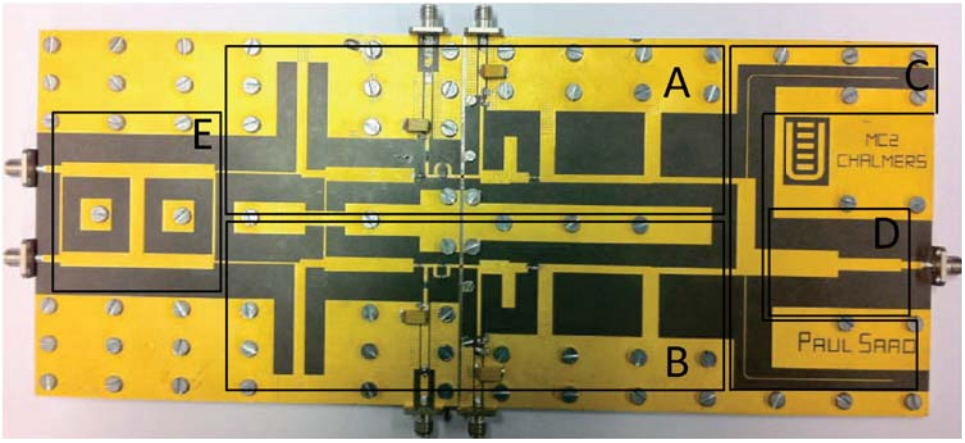

Fig. 2. Photos of the realized dual-band DPA. Box 'A' is the dual-band Main amplifier. Box 'B' is the dual-band Auxiliary amplifier. Box 'C' is the dual-band $\lambda/4$. Box 'D' is the network for the transformation from the 50 Ohm termination to the optimum output resistance. Box 'E' is the wide-band unbalanced input power splitter.

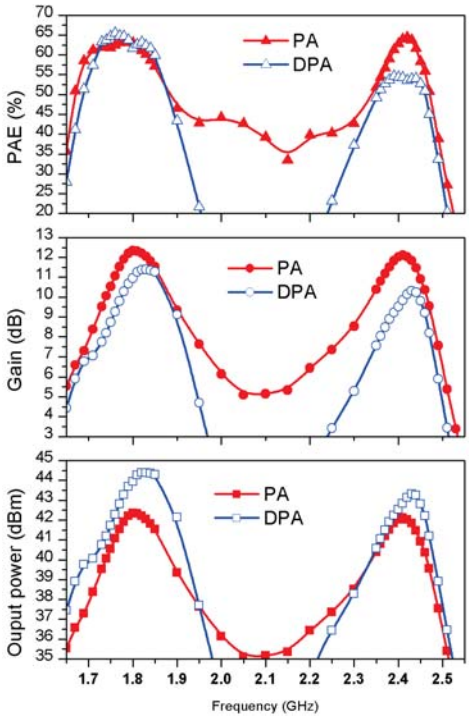

Fig. 3. CW measurements of dual-band PA and dual-band DPA.

concurrent mode, using a 10 MHz bandwidth LTE signal (PAR is about 7 dB) centered at 1.8 GHz and a 10 MHz bandwidth WiMAX signal (PAR is about 8.5 dB) centered at 2.4 GHz. The measured output spectrum, before and after digital-predistortion (DPD), at each band for both modules are shown in Fig. 4. These results are obtained imposing an average input power of 19 dBm and 22 dBm for the PA and the DPA, respectively. Moreover, the linearization was performed with the 2-D-DPD technique presented in [16]. The results reported in Fig. 4 show that standard DPD methods can be used to linearize dual-band concurrent modes to meet modern wireless communication system standards. Moreover, they demonstrate that the achieved linearity is independent from the architecture of the amplifier. Similar ACLR levels have been, in fact, registered from both modules. Finally, Table I summarizes the average performance of output power and PAE obtained from these experiments, highlighting the minimum ACLR level as well. It is possible to note that a 40% of PAE improvement has been reached from the DPA with respect to the PA, assuming the same operating condition. Such results demonstrate that the designed DPA can be satisfactory adopted to implement multi-band/multi-mode and efficient transmitter for both 2G, 3G, and 4G communication systems.

TABLE I
MEASURED AVERAGE OUTPUT POWER, AVERAGE PAE AND MINIMUM ACLR LEVEL, WITHOUT (W/O) AND WITH (W) DPD.

	Pout (dBm)		PAE (%)		ACLR (dBc)	
	w/o	w	w/o	w	w/o	w
PA	33.0	33.0	24.5	25.0	-34.3	-46.5
DPA	33.4	33.2	34.4	34.1	-29.0	-46.0

V. CONCLUSION

In this paper the design of a high peak efficiency dual-band power amplifier (PA) and how it is adopted as basic cell to implement a high average efficiency Doherty PA (DPA), achieving a dual-band/multi-mode and efficient transmitter concurrently operating at 1.8 GHz and 2.4 GHz, has been presented. Exhaustive experiments, based on both continuous wave and complex signals measures, have been carried out, demonstrating the capability of both modules to operate in concurrent mode reaching high efficiency levels with satisfactory linearity. Finally, the amount of PAE improvement that the DPA architecture can lead in 3G and 4G systems has been verified, highlighting its critical points in terms of gain reduction and sensitivity as well.

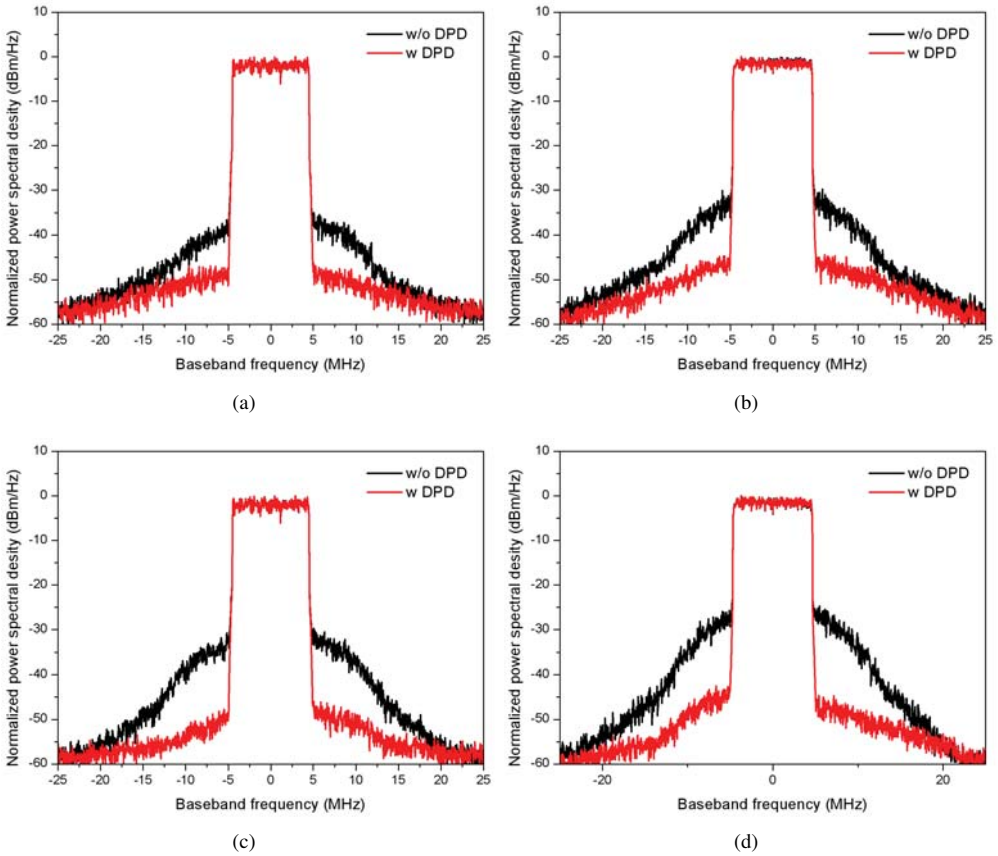

Fig. 4. Output signal spectrum, without (w/o) and with (w) DPD, of (a) dual-band PA by using a 10MHz LTE signal at center frequency of 1.8GHz, (b) dual-band PA by using a 10MHz WiMAX signal at center frequency of 2.4GHz, (c) dual-band DPA by using a 10MHz LTE signal at center frequency of 1.8GHz and (d) dual-band DPA by using a 10MHz WiMAX signal at center frequency of 2.4GHz. Both PA and DPA have been tested in concurrent mode.

ACKNOWLEDGMENT

This research has been carried out in the University of Roma Tor Vergata and in the GigaHertz Centre in a joint project financed by the Swedish Governmental Agency for Innovation Systems(VINNOVA).

REFERENCES

[1] K. Sahota, *RF Front End Requirements for 3G and Beyond*, IEEE Ultrasonics Symp., pp. 86-90, Oct. 11-14, 2010.

[2] G. Fettweis and E. Zimmermann, *ICT energy consumption trends and challenges*, Int. Symp. on Wireless Personal Multimedia Communications, 2008.

[3] J.N. LaPrade, J. Duthie, and D. Ferguson, *A Dual-Band Telemetry Transmitter for Broadcast Satellite Applications*, IEEE Military Communications Conference, pp. 141-145, Oct. 1984.

[4] P. Colantonio, F. Giannini, R. Giofré, and L. Piazzon, *A design technique for concurrent dual band harmonic tuned power amplifier*, IEEE Trans. Microw. Theory Tech., vol. 56, no. 11-II, pp. 2545-2555, Nov. 2008.

[5] Y. Ding, Y.X. Guo, and F.L. Liu, *High-efficiency concurrent dual-band class-F and inverse class-F power amplifier*, Electronics letters, vol. 47, no. 15, pp. 847 -849, July 2011.

[6] P. Saad, P. Colantonio, J. Moon, L. Piazzon, F. Giannini, K. Andersson, B. Kim, and C. Fager, *Concurrent Dual-Band GaN-HEMT Power Amplifier at 1.8 GHz and 2.4 GHz*, IEEE Wireless and Microw. Compon. Conf., accepted for publication within the proceedings of the conference, 2012.

[7] W. Doherty, *A new high efficiency power amplifier for modulated waves*, Proc. Inst. Radio Engineers, vol. 24, no. 9, pp. 11631182, Sep. 1936.

[8] P. Colantonio, F. Feudo, F. Giannini, R. Giofr, and L. Piazzon, *Design of a dual-band GaN Doherty amplifier*, Int. Conf. Microw. Radar Wireless Commun., pp. 14, Jun. 2010.

[9] X. Li, W. Chen, Z. Zhang, Z. Feng, X. Tang, and K. Mouthaan, *A concurrent dual-band Doherty power amplifier*, Asia-Pacific Microw. Conf. Proc., pp. 654657, Dec. 2010.

[10] W. Chen, S.A. Bassam, X. Li, Y. Liu, K. Rawat, M. Helaoui, F.M. Ghannouchi, and Z. Feng, *Design and linearization of concurrent dualband doherty power amplifier with frequency-dependent power ranges*, IEEE Trans. Microw. Theory Tech., to be published.

[11] P. Saad, P. Colantonio, L. Piazzon, F. Giannini, K. Andersson, and C. Fager, *Design of concurrent dual-band 1.8-2.4 GHz GaN-HEMT doherty power amplifier*, IEEE Trans. Microw. Theory Tech., accepted for publication within the next special issue on power amplifiers.

[12] C. Monzon, *A small dual-frequency transformer in two sections*, IEEE Trans. Microw. Theory Tech., vol. 51, no. 4, pp. 11571161, Apr. 2003.

[13] H. Zhang and K.J. Chen, *A stub tapped branch-line coupler for dualband operations*, IEEE Microw. Wireless Compon. Lett., vol. 17, no. 2, pp. 106108, Feb. 2007.

[14] P. Colantonio, F. Giannini, R. Giofre, and L. Piazzon, *The Doherty Power Amplifier, Advanced Microwave Circuits and Systems*, Vitaliy Zhurbenko (Ed.), ISBN: 978-953-307-087-2, InTech, 2010. Available from: http://www.intechopen.com/articles/show/title/the-doherty-power-amplifier

[15] M. Muraguchi, T. Yukitake, and Y. Naito, *Optimum design of 3-Db branch-line couplers using microstrip lines*, IEEE Trans. Microw. Theory Tech., vol. 31, no. 8, pp. 674678, Aug. 1983.

[16] W. Chen, S.A. Bassam, X. Li, Y. Liu, K. Rawat, M. Helaoui, F.M. Ghannouchi, and Z. Feng, *Design and linearization of concurrent dualband doherty power amplifier with frequency-dependent power ranges*, IEEE Trans. Microw. Theory Tech., vol. 59, no. 10, pp. 2537-2546, Oct. 2011.